ISSN 2616-5767 Vol.6, Issue 6: 5-16, DOI: 10.25236/AJETS.2023.060602

Research on second-order cone relaxation algorithm for multi-time linearization of distribution networks with distributed power sources

Zhu Meiyuan*, Ai Yongle

School of Electrical Engineering and Automation, Henan Polytechnic University, Jiaozuo, Henan, 454150, China
**Corresponding author: 3249937996@qq.com*

Abstract: *Distributed power supply connected to distribution network brings impact on system voltage distribution as well as tidal current analysis, which causes degradation of system power quality. For this reason, a system optimization model is needed to analyze and optimize system voltage and tidal current. The linearized second-order cone relaxation optimization algorithm for distribution networks with distributed power sources is proposed. First, the distribution network branch tide model is introduced to analyze the tide of the distribution network with distributed power supply access; based on this, the distributed distribution network tide optimization model is established. Secondly, the distributed distribution network tidal optimization model is simplified, and the multi-time second-order cone relaxation optimization algorithm is proposed for the non-convex nonlinearity in tidal analysis, and the segmental linearization is performed for the non-convex nonlinearity of capacitor bank and on-load regulator transformer. Finally, a modified IEEE33 node test system is used on the MATLAB simulation platform to verify the tidal optimization of this distributed distribution network tidal optimization system. The simulation results show that the tidal optimization algorithm can reasonably dispatch the output of on-load regulating transformers, capacitor banks and distributed power sources, effectively reduce the network loss and the voltage deviation of the grid.*

Keywords: *optimal power flow; mixed integer linear programming; segmented linear programming; multi-period SOCP algorithm*

1. Introduction

The access of distributed power supply to distribution network will change the distribution of power flow in distribution network and aggravate the voltage deviation of distribution network [1]. In order to rationally use the distributed power supply, stabilize the voltage deviation and realize the system energy saving, it is necessary to optimize the power flow distribution of the distribution network. Optimal power flow (OPF) is a non-convex nonlinear problem. It is difficult to find the optimal solution by using the interior point method, Newton method, heuristic intelligent algorithms such as genetic algorithm, particle swarm optimization [2] and other methods. Reference [3] used genetic algorithm to solve the multi-objective function, which can only solve the local optimal solution and cannot quantify the error between the global optimal solution. Based on this, the convex optimization of optimal power flow has received extensive attention.

The commonly used convex relaxation optimization techniques are semi-definite program (SDP) and second order cone program (SOCP) [4]. In the literature [5], the common convex relaxation techniques are introduced and their relaxation accuracy is compared. The conclusion is that although SDP has high solution accuracy, its solution speed is much lower than that of SOCP, and in large-scale test systems, the feasibility solution cannot be obtained. However, in the radial distribution network, the SOCP solution accuracy is the same as the SDP. Mixed integer linear programming (MILP) is a kind of nonlinear programming method, which is used to solve the optimization model with integer variables. Reference [6] used second-order cone relaxation and linearization techniques to transform the original non-convex nonlinear optimization into an approximate mixed integer linear program (MILP) solution, which reduced the optimality.

In this paper, SOCP algorithm is proposed to solve the non-convex nonlinear problem of multi-period power flow distribution in radial distribution network with distributed wind power generation. The IEEE-

ISSN 2616-5767 Vol.6, Issue 6: 5-16, DOI: 10.25236/AJETS.2023.060602

33 node test system is simulated and verified by MATLAB platform. The simulation results show that the power flow optimization algorithm can reasonably schedule the output of OLTC, CB and distributed power supply, effectively reduce the network loss and reduce the grid voltage deviation.

2. Power flow optimization model

For the distribution network with distributed wind power access, the system power flow distribution changes, and it is necessary to analyze and optimize the system model.

2.1. Distribution network branch power flow model

For the radial distribution network with distributed wind power generation, the distribution network contains n nodes and b branches, $N=\{1,2,...n\}$ represents the set of all nodes and $B=\{1,2,...b\}=\{(i,j)\}\subset(N\times N)$ represents the set of all branches. The branch flow model (BFM) is used to analyze the three-phase AC power flow of the system. The two-node power flow analysis model in the distribution network system is shown in Figure 1.

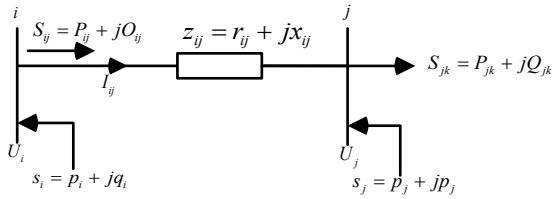

Figure 1: Two-bus system flow distribution

In Fig.1, I_{ij} represents the current flowing over the branch ij, $z_{ij}=r_{ij}+jx_{ij}$ represents the complex impedance of the branch ij, and $S_{ij}=P_{ij}+jQ_{ij}$ represents the complex power of the branch ij. $S_{jk}=P_{jk}+jQ_{jk}$ represent the complex power of branch jk, $s_i=p_i+jq_i$ and $s_j=p_j+jq_j$ represents the load power of nodes i and j.

Distribution network power flow model (BFM):

$$U_j^2=U_i^2-2(r_{ij}P_{ij}+x_{ij}Q_{ij})+(r_{ij}^2+x_{ij}^2)I_{ij}^2 \tag{1a}$$

$$p_j=P_{ij}-r_{ij}I_{ij}^2-\sum_{k:j\to k}P_{jk} \tag{1b}$$

$$q_j=Q_{ij}-x_{ij}I_{ij}^2-\sum_{k:j\to k}Q_{jk} \tag{1c}$$

$$U_i^2=\frac{P_{ij}^2+Q_{ij}^2}{I_{ij}^2} \tag{1d}$$

2.2. Distribution network power flow optimization model

The power supply security of the distribution network system is affected by the voltage offset. In order to make the system safe and reliable and save energy and reduce consumption, this paper takes the minimum voltage offset and the minimum line loss as the objective function expression of the distribution network optimization:

$$F_1=\min\Delta U=\sum_{i=1}^{N}\left(\frac{U_i-U_{Ni}}{\Delta U_{i\max}}\right)^2 \tag{2a}$$

$$F_2=\min P_{loss}=\sum_{ij\subset N}I_{ij}^2r_{ij} \tag{2b}$$

ISSN 2616-5767 Vol.6, Issue 6: 5-16, DOI: 10.25236/AJETS.2023.060602

In Equation (2), U_{Ni} represents the nominal value of *i* node voltage, $\Delta U_{i\max}$ represents the maximum voltage offset of *i* node.

Constraints: Distributed power access to the distribution network will affect the system voltage distribution and power flow size, so in the reactive power optimization not only need to consider their own voltage, current constraints, but also consider the power flow constraints. In addition, the constraints of capacitor banks and on-load tap changers should also be considered, as follows:

(1) Voltage and current constraints of distribution network:

$$U_{\min} \le U \le U_{\max} \tag{3a}$$

$$0 \le I \le I_{\max} \tag{3b}$$

(2) Generator constraints:

$$0 \le p_g \le p_{g\max} \tag{4a}$$

$$q_{g\min} \le q_g \le q_{g\max} \tag{4b}$$

(3) Power flow constraint:

$$\text{(1a)-(1d)} \tag{5}$$

(4) Distributed generation constraint

$$0 \le p_{wind} \le p_{wind\max} \tag{6}$$

(5) On-load Tap Changer (OLTC) constraints:

$$\Delta U_i^2 = t_m U_{OLTC}^2 \tag{7a}$$

$$t_m = \left(1 + \tau_m n_m^{tr}\right) \tag{7b}$$

$$n_m^{tr} \le n_m^{tr,\max} \tag{7c}$$

$$n_m^{tr} \in Z \tag{7d}$$

Equation (7a) is the relationship between the increment (ΔU_i) of node voltage U_i and the additional amount (U_{OLTC}) of OLTC voltage. The Equation (7b) is the relationship between OLTC ratio (t_m), tap position (n_m^{tr}) and tap step (τ_m). Equation (7c) is the constraint of OLTC tap position, Equation (7d) is the integer constraint of tap position, and Z is the integer set.

(6) Capacitor Bank (CB) constraints:

$$Q_i^{cp} = \Delta U_{CB}^2 b_i \tag{8a}$$

$$b_i = y_{c,i} n_i^{cp} \tag{8b}$$

$$n_i^{cp} \le n_i^{cp,\max} \tag{8c}$$

$$n_i^{cp} \in Z \tag{8d}$$

The Equation (8a) is the relationship between the admittance (b_i) of the capacitor bank and the reactive power (Q_i^{cp}) injected into the capacitor bank, and the voltage change caused by the access of the capacitor bank. The Equation (8b) is the relationship between the admittance value (b_i) of the capacitor bank and the number of units ($y_{c,i} \in R$), n_i^{cp} is the admittance value of a single capacitor bank; the Equation (8c) represents the constraint of capacitor bank admittance, $n_i^{cp,\max}$ is the upper limit of single capacitor bank admittance n_i^{cp} . The Equation (8d) is n_i^{cp} integer constraint, and Z is an integer

ISSN 2616-5767 Vol.6, Issue 6: 5-16, DOI: 10.25236/AJETS.2023.060602

set.

The power flow optimization of distribution network established above is a non-convex nonlinear optimization problem, and it is difficult to find the global optimal solution. Therefore, the second-order cone relaxation algorithm is used.

3. Nonlinear constraint condition processing

The Second Order Cone Program (SOCP) algorithm is a convex optimization algorithm with high efficiency and accuracy.

3.1 Second-order cone relaxation algorithm with nonlinear constraints

Defines the quadratic form variable X,

$$X=\begin{bmatrix}\dot{U}_i\\ \dot{I}_{ij}\end{bmatrix}\begin{bmatrix}\dot{U}_i\\ \dot{I}_{ij}\end{bmatrix}^H=\begin{bmatrix}\dot{U}_i(\dot{U}_i)^* & \dot{U}_i(\dot{I}_{ij})^*\\ \dot{I}_{ij}(\dot{U}_i)^* & \dot{I}_{ij}(\dot{I}_{ij})^*\end{bmatrix} \tag{9}$$

In Equation (9), let $l_{ij}=I_{ij}I_{ij}^*, W_{ij}=U_{ij}U_{ij}^*$ the power flow calculation formula (1) can be rewritten as.

$$W_j=W_i-2(r_{ij}P_{ij}+x_{ij}Q_{ij})+(r_{ij}^2+x_{ij}^2)l_{ij} \tag{10a}$$

$$p_j=P_{ij}-r_{ij}l_{ij}-\sum_{k:j\to k}P_{jk} \tag{10b}$$

$$q_j=Q_{ij}-x_{ij}l_{ij}-\sum_{k:j\to k}Q_{jk} \tag{10c}$$

$$W_i=\frac{P_{ij}^2+Q_{ij}^2}{l_{ij}} \tag{10d}$$

The above Equation (10d) is nonconvex, which is equivalent to the following inequality constraint and rank 1 constraint.

$$\begin{bmatrix}W_i & S_{ij}\\ S_{ij}^* & l_{ij}\end{bmatrix}\geq 0 \tag{11a}$$

$$rank\begin{bmatrix}W_i & S_{ij}\\ S_{ij}^* & l_{ij}\end{bmatrix}=1 \tag{11b}$$

In Equation (11), the inequality constraint is a positive semidefinite convex constraint, but the equality constraint (rank 1 constraint) is a non-convex constraint, which needs to be relaxed before solving.

The second-order cone relaxation is an approximate solution, and its principle diagram is shown in Figure 2.

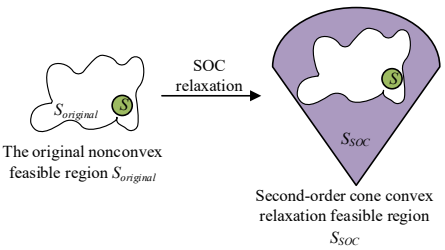

Figure 2: Sketch of second-order cone relaxation principle

ISSN 2616-5767 Vol.6, Issue 6: 5-16, DOI: 10.25236/AJETS.2023.060602

For non-convex and nonlinear problems cannot be solved directly, so the feasible region $S_{orginal}$ range is extended to the convex feasible region S_{SOC}, and the optimal solution S is the lower bound solution of the original non-convex problem. If $S \subset S_{SOC}$, the second-order cone convex relaxation is accurate, then S is the optimal solution of the original problem.

Then, according to Sylvester's criterion [7], the semidefinite constraint in (11) is exactly transformed into the second-order cone constraint as shown in (12).

$$\left\| \begin{matrix} 2W_i(i,i) \\ W_i(i,i) - W_i(j,j) \end{matrix} \right\|_2 \le W_i(i,i) + W_i(j,j) \tag{12a}$$

$$\left\| \begin{matrix} 2I_{ij}(i,i) \\ I_{ij}(i,i) - I_{ij}(j,j) \end{matrix} \right\|_2 \le I_{ij}(i,i) + I_{ij}(j,j) \tag{12b}$$

$$\left\| \begin{matrix} 2S_{ij}(i,i) \\ S_{ij}(i,i) - S_{ij}(j,j) \end{matrix} \right\|_2 \le S_{ij}(i,i) + S_{ij}(j,j) \tag{12c}$$

3.2. Piecewise linearization of OLTC and CB

The constraints (7) and (8) are non-convex nonlinear constraints, which makes it difficult to solve the optimization problem in polynomial time. By approximating non-convex constraints with piecewise linear programming (PWL) and mixed integer linear programming, OLTC and CB are modeled to obtain piecewise linear formulas [8].

The voltage relationship between OLTC nodes is:

$$\Delta W_i = t_{m,0}^2 W_{OLTC} + \sum_{p=1}^{K} \Delta U_p^m \tag{13a}$$

$$0 \le \Delta U_p^m \le \Delta t_{m,p} s_p^m W_{OLTC,\max} \tag{13b}$$

$$\Delta t_{m,p} \left(W_{OLTC} - \left(1 - s_p^m\right) W_{OLTC,\max} \right) \le \Delta v_p^m \le \Delta t_{m,p} U_{OLTC} \tag{13c}$$

$$s_{p+1}^m \le s_p^m, p = 1,2,...K-1. \tag{13d}$$

In Equation (13), $W_{OLTC} = U_{OLTC}^2$, $\Delta U_p^m = \Delta t_{m,p} W_{OLTC}$, $\Delta t_{m,p} = t_{m,p}^2 - t_{m,p-1}^2$, $\{ t_{m,0}, t_{m,1}, t_{m,2} \dots t_{m,R} \}$ represents the fixed tap position of OLTC connected by branch m; binary variable $\{ s_1^m, s_2^m, \dots s_k^m \}$ and $s_p^m \ge s_{p+1}^m$, $p = 1, 2, \dots K-1$ represents the running state of OLTC branch, if $s_p^m = 0$, then $\Delta v_p^m = 0$, if $s_p^m = 1$, then $\Delta U_p^m = \Delta t_{m,p} W_{OLTC}$.

The relationship between the capacitor bank admittance (b_i) and the reactive power injected into the capacitor bank (Q_i^{cp}) is:

$$Q_i^{cp} = \sum_{P=1}^{K} Q_{i,p}^s \tag{14a}$$

$$0 \le Q_{i,p}^s \le u_p^i W_{CB,\max} b_{i,p} \tag{14b}$$

$$b_{i,p} \left(W_i - \left(1 - u_p^i\right) W_{CB,\max} \right) \le Q_{i,p}^s \le W_i b_{i,p} \tag{14c}$$

$$u_{p+1}^i \le u_p^i, p = 1,...,K-1. \tag{14d}$$

In Equation (14), $W_i = U_i^2$, $W_{CB,\max} = U_{CB,\max}^2$, $Q_{i,p}^s$ is the reactive power of a single capacitor

ISSN 2616-5767 Vol.6, Issue 6: 5-16, DOI: 10.25236/AJETS.2023.060602

bank ; U_p^i represents the operating state of the shunt capacitor. $\{ b_{i,1}, \ b_{i,2} \ \ldots \ b_{i,K} \}$ is the admittance value of the controllable capacitor bank at node *i*, $Q_{i,p}^s$ represents the product value of W_i and $b_{i,p}$. The binary $\{ u_1^i, \ u_2^i \ \ldots \ u_K^i \}$ represents the operating state of the capacitor bank at node *i*.

4. Dynamic multi-period SOCP algorithm

4.1. Dynamic multi-period SOCP-OPF model establishment

Single-period optimization is to optimize the distribution network with constant system load demand, but in fact the load of the distribution network is changing. For the distribution network with distributed power supply, that is, the active distribution network, generally 24 hours is a load cycle. According to the load change and the power generation status of the distributed power supply, a load cycle can be divided into multiple periods. If a load cycle is divided into too many periods, the OLTC switching times are too many, resulting in wear and tear, and the calculation amount is cumbersome and complicated, and the result cannot be obtained. If too few time periods are divided, the calculation results will be unreliable, so the appropriate number of time periods should be selected. In this paper, each hour is selected as a period of time, and a load cycle is divided into 24 periods. In a load cycle, the dynamic multi-period MISOCP-OPF model is as follows:

$$F_1^{'} = \min \sum_{t=1}^{T} \left(\sum_{i=1}^{N} (\frac{U_{i,t} - U_{Ni,t}}{\Delta U_{i\max}})^2 \right) \tag{15a}$$

$$F_2^{'} = \min \sum_{t=1}^{T} \left(\sum_{ij \subset N} I_{ij,t}^2 r_{ij} \right) \tag{15b}$$

The power flow constraint condition in *t* period is:

$$W_{j,t} = W_{i,t} - 2(r_{ij} P_{ij,t} + x_{ij} Q_{ij,t}) + (r_{ij}^2 + x_{ij}^2) l_{ij,t} \tag{16a}$$

$$p_{j,t} = P_{ij,t} - r_{ij} l_{ij,t} - \sum_{k:j \to k} P_{jk,t} \tag{16b}$$

$$q_{j,t} = Q_{ij,t} - x_{ij} l_{ij,t} - \sum_{k:j \to k} Q_{jk,t} \tag{16c}$$

Second-order cone relaxation constraint in *t* period:

$$\left\| \begin{matrix} 2W_{i,t}(i,i) \\ W_{i,t}(i,i) - W_{i,t}(j,j) \end{matrix} \right\|_2 \le W_{i,t}(i,i) + W_{i,t}(j,j) \tag{16d}$$

$$\left\| \begin{matrix} 2I_{ij,t}(i,i) \\ I_{ij,t}(i,i) - I_{ij,t}(j,j) \end{matrix} \right\|_2 \le I_{ij,t}(i,i) + I_{ij,t}(j,j) \tag{16e}$$

$$\left\| \begin{matrix} 2S_{ij,t}(i,i) \\ S_{ij,t}(i,i) - S_{ij,t}(j,j) \end{matrix} \right\|_2 \le S_{ij,t}(i,i) + S_{ij,t}(j,j) \tag{16f}$$

Node voltage, branch current, power generation equipment, OLTC and CB constraints in *t* period:

$$W_{\min} \le W \le W_{\max} \tag{16g}$$

$$0 \le l \le l_{\max} \tag{16h}$$

$$(4),(6),(13),(14) \tag{16i}$$

In practical processing, considering the second-order cone convex relaxation error. Error can be calculated by formula (17).

ISSN 2616-5767 Vol.6, Issue 6: 5-16, DOI: 10.25236/AJETS.2023.060602

$$Error = l_{ij}W_i - P_{ij}^2 - Q_{ij}^2 \tag{17}$$

4.2. Dynamic multi-period SOCP algorithm flow

In the above multi-period dynamic power flow optimization model, the control variables not only involve flexible resources such as generators and wind turbines, but also discrete resources such as OLTC and CB. For the static power flow optimization model, the system impedance, power load demand and other parameters are given. Given the objective function; the upper and lower bounds of system voltage and current, and the upper and lower bounds of capacity of generators, wind turbines and capacitor banks. By using the second-order cone convex relaxation algorithm, the non-convex nonlinear problem that cannot be directly solved is transformed into a solvable model. Through the YALMIP simulation software package, a single-period optimization model is established. Considering the change of system load demand, it is transformed into a multi-period optimization model. Finally, the Gurobi solver is called to solve the model. The specific algorithm flow chart is shown in Figure 3.

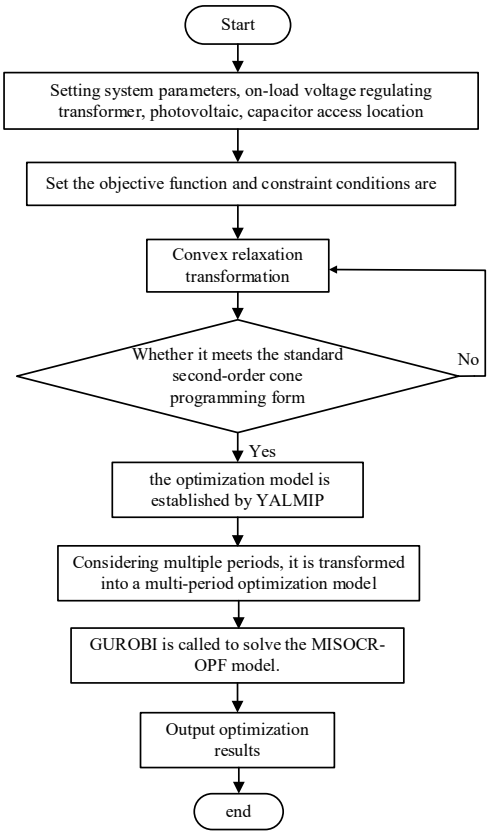

Figure 3: Flow chart of multi-time optimal power flow algorithm for radiation type distribution network

5. Simulation analysis

5.1. Select the node test system

The IEEE-33 standard node test system is selected as the power reference value and voltage reference value. The on-load voltage regulating transformer is indirectly connected at 33 and 1 nodes. The voltage regulating range is 0.9 ~ 1.1, and the voltage regulating step is 0.0125, with a total of 17 grades. The wind turbine is connected to the 17 and 32 nodes, and the maximum capacity is taken; the capacitor bank is connected at 5 and 15 nodes, and the capacitor capacity of each group is taken, a total of 5 groups. The IEEE-33 standard node test system is shown in Figure 4, and the 24-hour active and reactive loads of each node are shown in Figure 5.

ISSN 2616-5767 Vol.6, Issue 6: 5-16, DOI: 10.25236/AJETS.2023.060602

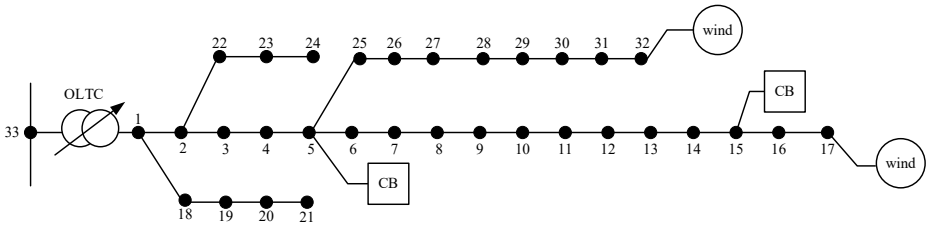

Figure 4: IEEE-33 standard node test system

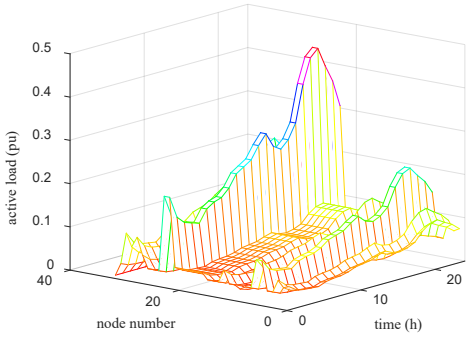

Figure 5: (a) 24-hour load active power output graph

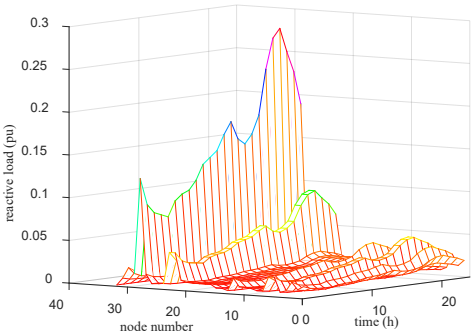

Figure 5: (b) 24-hour load reactive power output graph

Figure 5: 24-hour load active and reactive power output graph

5.2. Analysis of simulation results

Table 1: Results of 11 iterations

iteration times	1	2	3	4	5	6	7	8	9	10	11
F_1(total voltage deviation /pu)	1.404	1.365	1.366	1.366	1.362	1.371	1.366	1.366	1.366	1.366	0.491
F_2(total active network loss/pu)	0.372	0.374	0.374	0.375	0.374	0.373	0.375	0.375	0.375	0.375	12.210

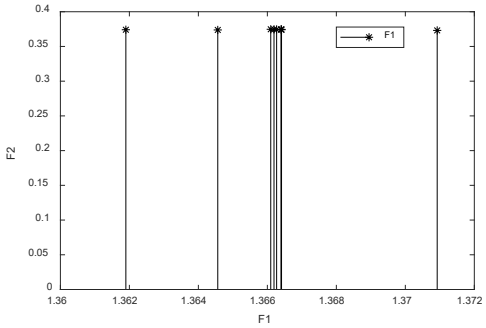

Figure 6: Dual-objective Pareto front

ISSN 2616-5767 Vol.6, Issue 6: 5-16, DOI: 10.25236/AJETS.2023.060602

The MATLAB example simulation is carried out on the computer with 2.2GHz processor and 16GB running memory. The number of iterations of the SOCP algorithm is set to 11, and the simulation results are shown in Table 1. According to the data of table 1, the voltage deviation of the first time is the largest, and the network loss of the 11 th time is the largest. When solving the Pareto front, in order to make the data more accurate, the first and 11th results are removed, and only the results of the middle 9 times are retained. The Pareto front found is shown in Figure 6.

The optimal point of the target is obtained at the fifth simulation, that is, F1 (total voltage offset) is 1.362 pu, F2 (total active network loss) is 0.374 pu, and the objective function takes the optimal value. It can be seen from Table 1 that compared with the initial power flow calculation node voltage deviation, the voltage deviation value of the fifth iteration is reduced by 0.042 pu.

The node voltage distribution in the 24-hour period corresponding to the optimal objective function is shown in Figure 7 (a). In order to intuitively analyze the distribution of node voltage, the relationship between each node voltage and the node sequence number is shown in Figure 7 (b). The relationship between each node voltage and each moment is shown in Figure 7 (c).

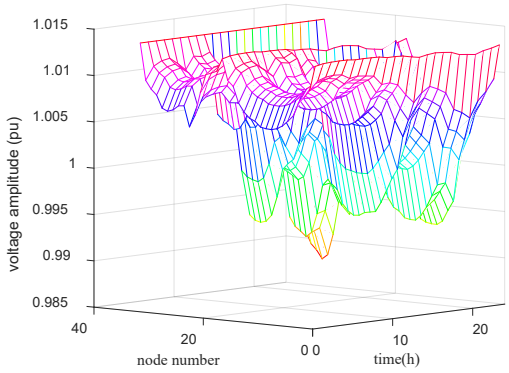

(a) 24-hour bus voltage distribution

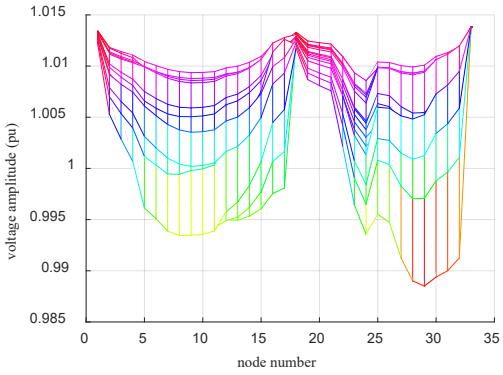

(b) Voltage distribution of each bus

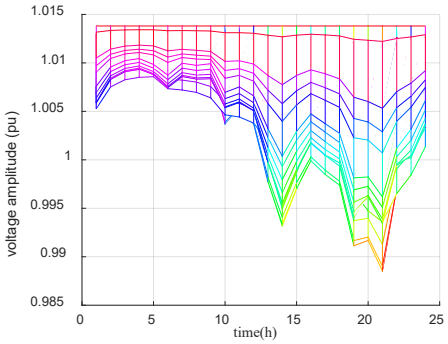

(c) Bus voltage distribution by time period

Figure 7: Bus voltage distribution

According to Figure 7 (b), 33 nodes as the root node, the node voltage is the highest (1.014pu); secondly, due to the access of wind turbines, the node voltage at 17 nodes and 32 nodes is raised. It can be seen from Fig.7 (c) that from 19h to 22h, the voltage is low due to the high load demand.

ISSN 2616-5767 Vol.6, Issue 6: 5-16, DOI: 10.25236/AJETS.2023.060602

Under the optimal objective function, the comparison diagram of active power output and load active power demand is shown in figure 8 (a), the comparison diagram of reactive power output and load reactive power demand is shown in figure 8 (b), the output of wind turbine is shown in figure 8 (c), and the output of capacitor bank is shown in figure 8 (d).

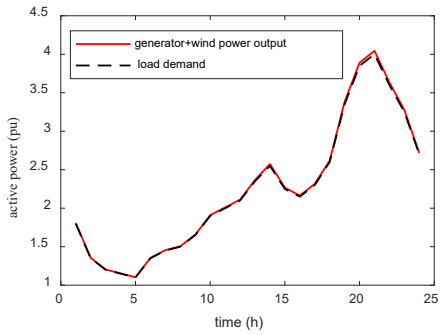

(a) Comparison of active power output and active load demand

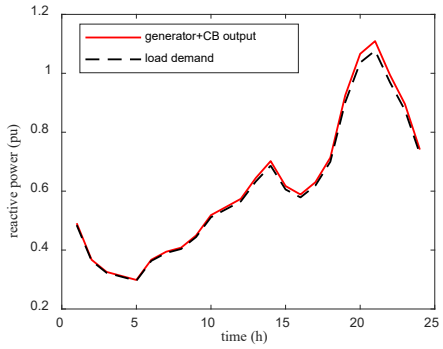

(b) Comparison of reactive power output

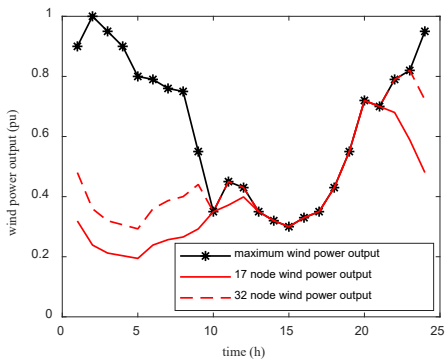

(c) 24-hour wind generator output power

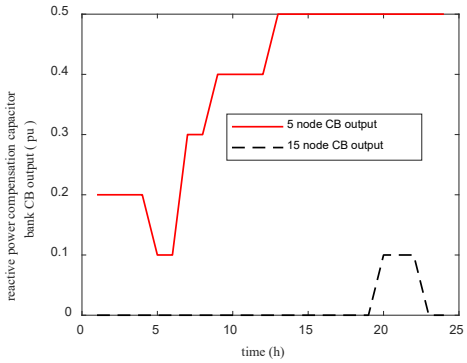

(d) 24-hour CB output power

Figure 8: Generator, wind generator, CB output power

It can be seen from Figure 8 (a) that the output power of the generator at 33 nodes basically changes with the change of load demand. There will be a large active output between 19h and 22h, which is

ISSN 2616-5767 Vol.6, Issue 6: 5-16, DOI: 10.25236/AJETS.2023.060602

basically consistent with the load active demand. The difference mainly comes from the active power provided by the wind turbine. Reactive power is the same. It can be seen from Figure 8 (c) that between 19h and 22h, due to the large load demand, in order to maintain the voltage level, the output of the wind turbine is the maximum. From Figure 8 (d), it can be seen that the node voltage at the 5 node is low, and the CB compensation voltage is connected, and its output changes with the change of voltage. The load demand becomes larger at 20 h, and only the 5 node CB output cannot meet the node voltage level. At this time, under the condition that the 5 node CB maintains the maximum output, the CB at the 15 node begins to output and continues to lift the system voltage.

Under the optimal objective function, the proportion of active power loss in 24 periods to the total active power output of power generation is shown in Fig. 9.

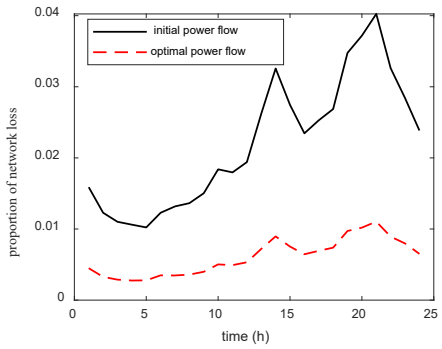

Figure 9: Active network loss ratio by time period

It can be seen from Figure 9 that compared with the proportion of the initial power flow active power loss to the total active power output of the power supply, the proportion is greatly reduced under the optimal objective function. That is to say, the total active power loss of the system is reduced from 22.94 % to 14.47 % by SOCP algorithm.

Under the optimal objective function, the relaxation error of the second-order cone convex relaxation algorithm can be calculated by formula (17) as shown in Figure 10.

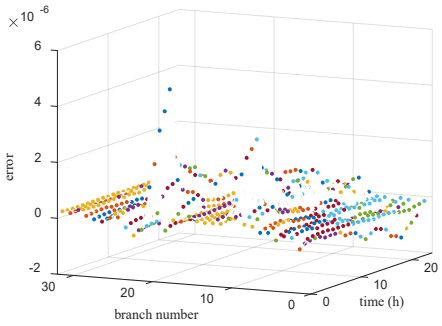

Figure 10: SOCP algorithm slackening error

It can be seen from Fig.10 that the multi-period SOCP algorithm has a solution error of 10-6 orders of magnitude in solving non-convex nonlinear problems, which fully meets the accuracy requirements.

The solution time of dynamic multi-period SOCP is compared with other algorithms as shown in Table 2.

Table 2: Comparison of dynamic multi-period SOCP and krill swarm algorithm [9]

solving algorithm	iteration times	active network loss (%)	minimum node voltage (pu)	solving time
krill swarm algorithm	12	34.75	0.956	>30min
Multi-period SOCP algorithm	4	14.47	1.024	9.74s

From Table 2, it can be seen that compared with the krill herd algorithm, the multi-period MISOCP algorithm has fewer iterations, shorter solution time, lower active network loss, and higher minimum

ISSN 2616-5767 Vol.6, Issue 6: 5-16, DOI: 10.25236/AJETS.2023.060602

voltage. The second-order cone relaxation algorithm has obvious advantages in solving nonlinear and non-convex problems.

6. Conclusion

Aiming at the optimal power flow problem of three-phase radial distribution network, a multi-period SOCP algorithm is proposed to solve the non-convex nonlinear problem in three-phase AC OPF and the optimization problem with the participation of wind power, OLTC and CB. By MATLAB simulation, the conclusions are as follows.

(1) The multi-period SOCP algorithm is used to solve the OPF. Under the premise of ensuring the solution accuracy of 10-6 orders of magnitude, the total active network loss of the system is reduced from 22.94 % under the initial power flow to 14.47 %.

(2) The active power output of wind turbine, the reactive power output of CB and the total offset of node voltage are reduced by 0.042 pu, which improves the power quality.

Acknowledgements

Project Fund: 2017 Henan Provincial Science and Technology Research Plan Project "Research on Key Technologies of High Power Micro Grid Energy Storage Converter" Project No.: 172102310569.

References

[1] Zhou L, Wang J, Xie L, et al. Multi-objective reactive power optimization of distribution network with distributed generation [J].Journal of Chongqing University of Posts and Telecommunications (Natural Science Edition), 2022,34 (05) : 818-827.

[2] Sun S Q, Wu C Y, Yan W L, et al. Optimal power flow calculation based on particle swarm with random decay factor [J]. Power System Protection and Control, 2021, 49(13): 43-52.

[3] Rong Y J, Feng H C, Song L W, et al. Distribution grid reactive power optimization based on adaptive genetic algorithm containing photovoltaic power supply [J]. Electrical and Energy Efficiency Management Technology, 2020 (11): 85-91.

[4] Zhang R, Li T C, Li X M, et al. Distributed voltage reactive power optimization in distribution networks considering equipment action losses [J]. Power System Protection and Control, 2021, 49(24): 31-40.

[5] Lin Z, Hu Z C, Song Y H. A review of convex relaxation techniques for optimal flow problems [J]. Chinese Journal of Electrical Engineering, 2019, 39(13): 3717-3728.

[6] Zhang X, Yao L, Chen C, et al. A two-stage robust optimization model for hybrid AC-DC distribution network reconfiguration with reactive power optimization synergy [J]. Power Grid Technology, 2022, 46(03): 1149-1162.

[7] Xu T R, Ding T, Li L, et al. A second-order cone relaxation model for adapting reactive power optimization in three-phase unbalanced active distribution networks [J]. Power System Automation, 2021, 45(24):81-88.

[8] Z. Yang, A. Bose, H. Zhong, etc. "Optimal reactive power dispatch with accurately modeled discrete control devices: a successive linear approximation approach," IEEE Trans. Power Syst, vol. 32, no. 3, pp. 2435–2444, 2017.

[9] Gao J L, Song S, Wang L Y, et al. Reactive power optimization of active distribution network based on improved krill herd algorithm [J].Journal of Jilin University (Information Science Edition), 2022,40 (06) : 954-962.